Hindawi
International Journal of Antennas and Propagation
Volume 2023, Article ID 8894404, 10 pages
https://doi.org/10.1155/2023/8894404

Research Article

Design of Miniaturized FSS with High Angular Stability Utilizing a Novel Closed Loop

Wei Li, Fengshuo Zhang, Ying Suo, Zhe Jiang, and Jinghui Qiu

School of Electronics and Information Engineering, Harbin Institute of Technology, Harbin, China

Correspondence should be addressed to Ying Suo; suoyingsing@126.com

Received 18 December 2022; Revised 5 June 2023; Accepted 9 June 2023; Published 12 July 2023

Academic Editor: Rajkishor Kumar

In this paper, we propose a miniaturized 2.5-dimensional (2.5D) frequency selective surface (FSS) structure with high angular stability. A novel closed-loop FSS is formed by combining the Jerusalem cross (JC) structure with the conventional rectangular closed loop using vias. This approach further enhances the coupling performance of the FSS and thus achieves miniaturized design. The unit cell size of the proposed FSS is $0.019\lambda_0 \times 0.019\lambda_0$ at the resonant frequency, and the metal is printed on a dielectric substrate with a thickness of $0.003\lambda_0$. The proposed FSS has a resonant frequency of 850 MHz and exhibits band-stop characteristics. It is insensitive to the incident angle with a good operating performance in both the TE and TM wave modes. Therefore, it can be well used as an electromagnetic shield for the GSM 850 band. In order to facilitate the rapid analysis and design of the FSS, the equivalent circuit model is further analyzed and established, and values of the corresponding lumped components are derived. In addition, a prototype FSS is fabricated using printed circuit board technology and is tested in a microwave anechoic chamber. The full-wave analysis simulation, equivalent circuit model simulation, and practical measurement results reflect a high level of consistency.

1. Introduction

Frequency selective surfaces have gained more and more attention as they are widely used in electromagnetic shielding, absorbers, antennas, and radomes [1–4]. The FSS consists of a periodic structure with different cell structures. Conventional FSSs are usually printed on single sides of the dielectric substrate on two-dimensional structures, but such structures are not sufficient to meet the demand for miniaturization of the FSS size. For FSSs, the physical size is not infinite planes in design. In order to achieve a better performance, it is necessary to arrange more FSS cells on the finite size, especially for low frequency bands, and the demand for miniaturization of FSSs is already proposed [5]. To reduce the size of FSS, a lot of methods have been proposed, such as three-dimensional (3D) technology [6] or hybrid 2D and 3D technology [7]. However, 3D processing is more difficult and increases the thickness of the FSS [8]. Therefore, the 2.5D FSS is gaining more and more attention. The conventional 2D planar structure is a horizontal X-Y plane, and when vias are added, the vertical Z-direction plane is also utilized. The vertical vias will further increase the metal density in the FSS, making it easy to achieve miniaturization. The PCB production process does not need to be changed at this time but is still in the form of traditional planar printing; so, the FSS structure with via inserted is called the 2.5D FSS [9, 10]. The FSS generally uses two classical structures, the JC and the closed loop. In recent years, improved 2.5D structures on these two structures have been proposed [11]. The strong coupling effect is verified by adding vias to the conventional JC FSS to form the 2.5D FSS [12]. The 2.5D structure is able to increase the capacitance and inductance of the cell by connecting both sides of the dielectric substrate using vertical vias [13]. Therefore, the 2.5D structure can reduce the size of the FSS and achieve better oblique incident angular stability.

Recently, various 2.5D FSS structures with excellent performance have been proposed, and miniaturized FSSs can be achieved using the JC structure with many vias [14]. Meandering lines are utilized in the JC FSS to further reduce

the resonant frequency to achieve miniaturization [15]. Also, some methods can be regarded as improvements to the closed loop or loop structure [16, 17]. The FSSs are limited by structural features and only have a few vias added to initially achieve a 2.5D structure with miniaturization [18, 19]. To overcome this problem, an FSS that utilizes a knitted structure to insert more vias is proposed [20]. On the other hand, the electrical size of the FSS can be reduced by using an inward-convoluted loop structure with the metallic strips, which can largely enhance the mutual coupling between metals [21]. Several closed-loop FSSs with fractal structures have been proposed in order to maximize the use of the dielectric layer space [22, 23]. In addition, it is difficult to reduce the miniaturization size and maintain angular stability to more than 85°.

In this paper, a closed-loop 2.5D FSS for electromagnetic shielding is proposed. The novel closed-loop structure with a strong coupling performance is presented to achieve miniaturization of the cell and reduction of the profile height, as well as high angular stability. In addition, the FSS is converted into an equivalent circuit model for verification and analysis. The proposed FSS is fabricated and measured to verify the designed specifications.

2. Unit Cell Design

The structure of the proposed FSS unit cell is shown in Figure 1(a). It is a symmetrical structure with the metal printed on both sides of an FR4 dielectric substrate which relative permittivity is 4.6, loss tangent is 0.019, and thickness is 1.2 mm. The top and bottom views of the FSS are shown in Figures 1(b) and 1(c), respectively. In the above figure, the brown part represents the metal, the dielectric is filled with yellow color, and the vias are shown using black. The metal on the surface is a novel closed-loop structure which can be seen as a combination of a loop-back rectangular ring and a JC structure with a solder ring, where the metal strip is connected to the vias. This structure introduces more vias, allowing for enhanced coupling.

The FSS, as a periodic structure, in general has a cell size approximating $\lambda/2$, which is relatively large. Therefore, in order to meet the needs of practical applications, it needs to be miniaturized at the design time. The FSS resonant frequency can be expressed as follows: L and C represent the equivalent inductance and capacitance; so, it is necessary to enhance the equivalent inductor and capacitor to make a lower working frequency at the same physical size in order to achieve miniaturization. The cell design of the proposed structure has evolved as follows. As a closed-loop type FSS, the initial structure is shown in Figure 2(a). Each cell consists of a closed loop, which has a small metal length in the loop and a large gap between the metals; so, the equivalent capacitor and inductor are small. Furthermore, a 2.5D structure can be developed using vias, where the length of the loop metal is further increased, as shown in Figure 2(b). Then, the meandering line is utilized, and the metal strips in Figure 2(c) are spiraled inward to increase the length, while additional capacitance is inserted between the closely spaced metal strips. In order to increase the number of vias, the traditional closed-loop structure is combined with the JC structure to form a new closed-loop structure, i.e., the proposed structure in this paper, which is shown in Figure 2(d). The novelty lies in the insertion of a few vias in the long metal strip of the JC structure and combining this JC structure with the existing closed-loop structure to form a new closed loop, which achieves maximum miniaturization.

Full-wave electromagnetic simulations are performed, using unit cell boundary conditions and floquet ports for excitation. Figures 3(a) and 3(b) show the simulation results of the FSS under two different polarization, such as the TE and TM modes with different incident angles, respectively. From them, it can be seen that the FSS can be regarded as a band-stop filter with a resonant frequency of 850 MHz. The maximum amplitude of the transmission coefficient is 23.3 dB when the incident angle is 0 degree, which means that only 6.8% of the energy can pass through the FSS. GSM850 is a relatively important frequency band for mobile communication, and many smart terminals support this band, so the proposed FSS can better protect the relevant devices from interference in this band. Moreover, it is demonstrated that the transmission coefficients with different incident angles of the proposed FSS is highly stable, and its resonant frequency remains stable at incident angles as high as 85°. So, its resonant frequency shift is almost negligible. Also, the performance of the proposed FSS is in excellent agreement in both the TE and TM modes, where the resonant frequency is 850 MHz at both modes. The resonant bandwidth of the TE mode is widened with the increase of the incident angle because the wave impedance changes with the angle, while the TM mode is the opposite. Also, Figure 3(c) verifies the polarization stability of the FSS, as the transmission coefficient and resonant frequency are almost unchanged when the polarization angle is from 0 to 60 degrees, which illustrates the good polarization stability of the FSS.

The FSS can essentially be considered as a spatial filter and, therefore, its operating frequency is the most important characteristic. It is worth mentioning that the FSS and the absorber have some similarities. Both the microwave absorber and band-stop FSS are a form of metasurface, which is essentially a periodic structure and thus has unique electromagnetic characteristics. Also, both can achieve the effect of rejection electromagnetic waves, which is also expressed as $S21 << 1$. However, there are differences in the design idea that both S11 and S21 of microwave energy absorbers are small and will neither reflect nor transmit electromagnetic waves but will preserve the energy of electromagnetic waves as losses in the medium or metal [24]. The FSS, on the other hand, has a larger S11, which is very close to 1, which reflects most of the energy back. For this design applied for electromagnetic shielding on other bands, its resonant frequency needs to be changed. The change in resonant frequency can be achieved by modifying some parameters of the structure.

Considering both dielectric and structural parameters separately, the relative permittivity and thickness of the substrate as well as the cell gap are modified. Multiple sets of parameters are selected to analyze, and the obtained results

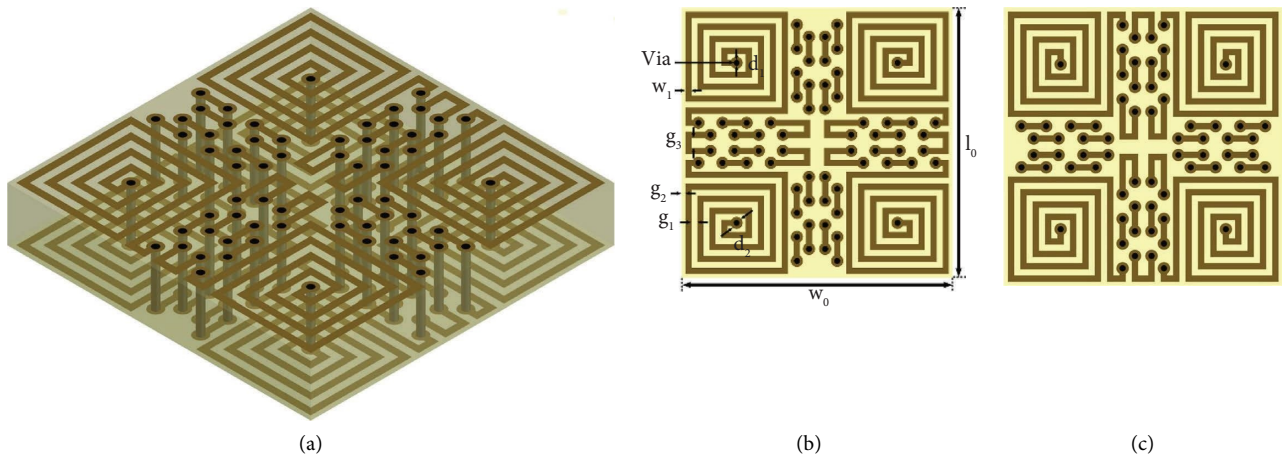

(a) (b) (c)

Figure 1: Structure of the proposed FSS unit cell. When the resonant frequency is 850 MHz, the optimized parameters are as follows: $w_0 = 6.75$ mm, $l_0 = 6.75$ mm, $w_1 = 0.15$ mm, $d_1 = 0.15$ mm, $d_2 = 0.3$ mm, $g_1 = 0.15$ mm, $g_2 = 0.1$ mm, $g_3 = 0.25$ mm, and the cell size is 6.75 mm × 6.75 mm. (a) 3D view. (b) Top view. (c) Bottom view.

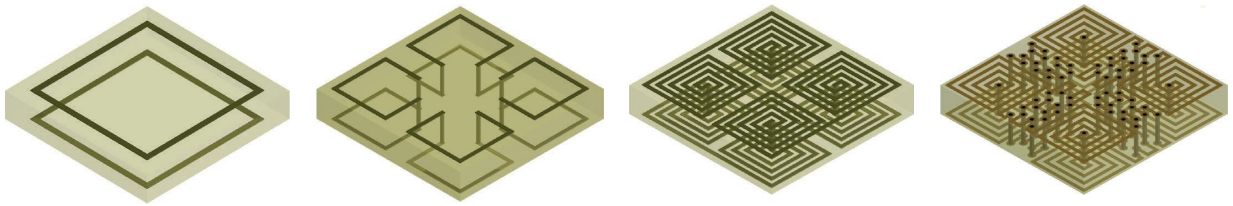

(a) (b) (c) (d)

Figure 2: Miniaturization ideas for the proposed FSS.

are shown in Figure 4. It is demonstrated that if the larger relative permittivity is chosen, the lower working frequency of this FSS operates, and the thicker dielectric substrate is, the lower the working frequency is.

3. Equivalent Circuit Modeling

In order to further understand the operation of the proposed FSS, it is necessary to analyze its equivalent circuit. The equivalent circuit model (ECM), similar to a filter system, can be considered as an LC resonant circuit. The equivalent circuit, similar to the filter in the circuit, can be considered as an LC resonant circuit, and the equivalent circuit can be constructed by analyzing the placement of inductors and capacitors. For this purpose, the current and electric field distributions of the model in Figure 1 are analyzed. The current and electric field distributions at the bottom with TE mode excitation in the full-wave simulation are shown in Figures 5(a) and 5(b), respectively. In this case, the region with a high surface current density can be equated to an inductor, while the region with a high density of electric field distribution can be considered as a capacitor. The figure shows that the current density is higher at the metal strip and the electric field intensity is higher at the metal and the gap over the hole; so, it can also be concluded that the metal part can be considered as inductance, while the gap part can be considered as the capacitive region.

Based on the abovementioned equivalence principle for the electric field and the current concentration region, Figure 5(c) shows the relative positions of the inductors and capacitors on the FSS, i.e., L_1 and L_3 are the inductors equated by the ring metal strip, C_1 and C_3 are equivalent capacitors by the gap between the ring metal strips, L_2 is the inductor through the vias, C_2 is the capacitor between the vias, and C_4 is the capacitance contributed by the JC structure in the middle of the cell. This makes it possible to convert the FSS into an ideal equivalent circuit model as shown in Figure 6(a). Since the FSS will be placed in free space during usage, the ports on both sides of the equivalent circuit are free space, i.e., its impedance is $Z0 = 377$ Ohm. The dielectric substrate of the FSS can be regarded as a section of transmission line with characteristic impedance, which is represented as Z_{sub} in the equivalent circuit. In addition, the LC is the ideal component in the equivalent circuit for easier analysis. Figure 6(a) is an equivalent circuit model that can actually describe the operation of the FSS based on the distribution of current and the electric field, which realistically shows the actual contribution of capacitance and inductance in the FSS structure, but it is not helpful to extract the specific value of the LC due to its more components. Considering that the LCs in the model of Figure 6(a) are all ideal components, the series inductors L_1 and L_3 and capacitors C_1 and C_3 can be directly simplified, i.e., there are: $L_1' = L_1 + L_3$ and $C_1' = (C_1 * C_2)/(C_1 + C_2)$.

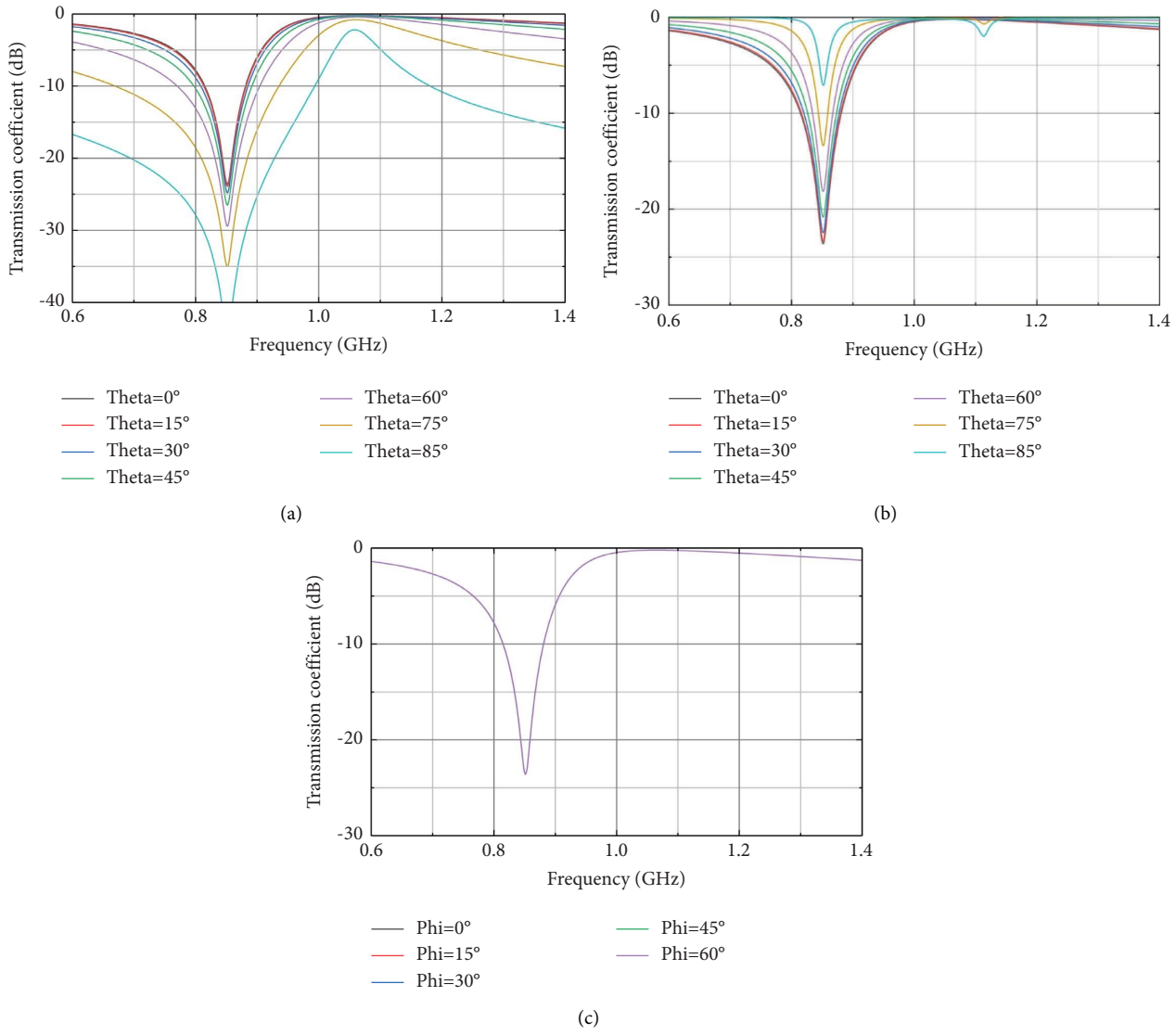

Figure 3: Simulated transmission coefficients of the proposed FSS. (a) Various incident angles of the TE mode. (b) Various incident angles of the TM mode. (c) Various polarization angles.

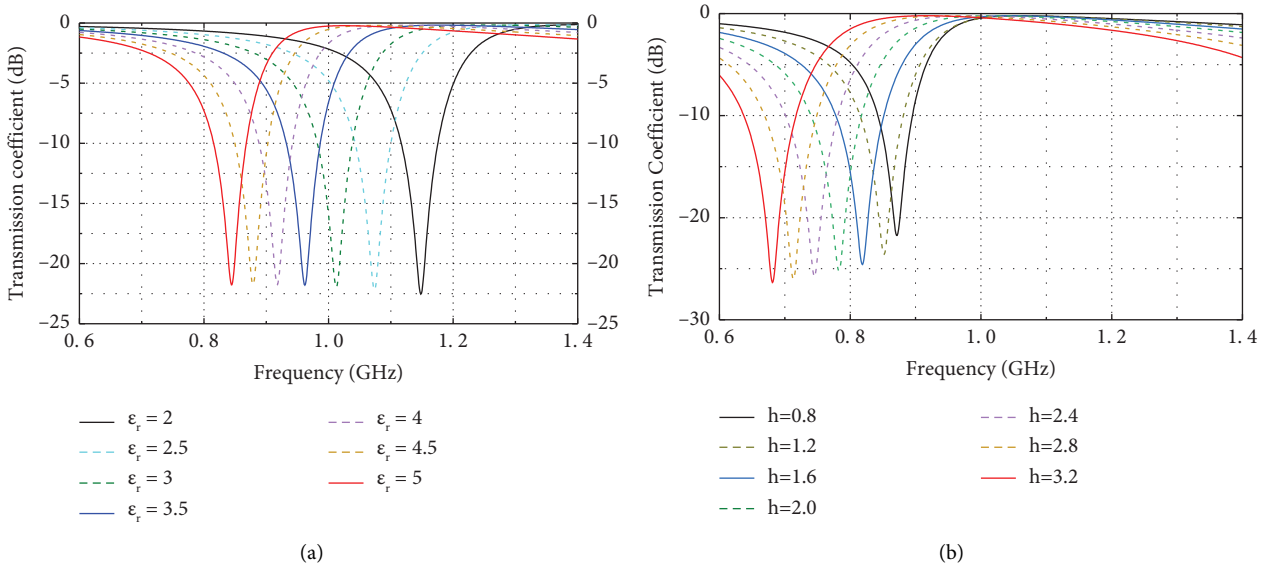

Figure 4: Influence of parameters on the transmission coefficient. (a) Different relative permittivity ε_r. (b) Different thickness of dielectric substrate h.

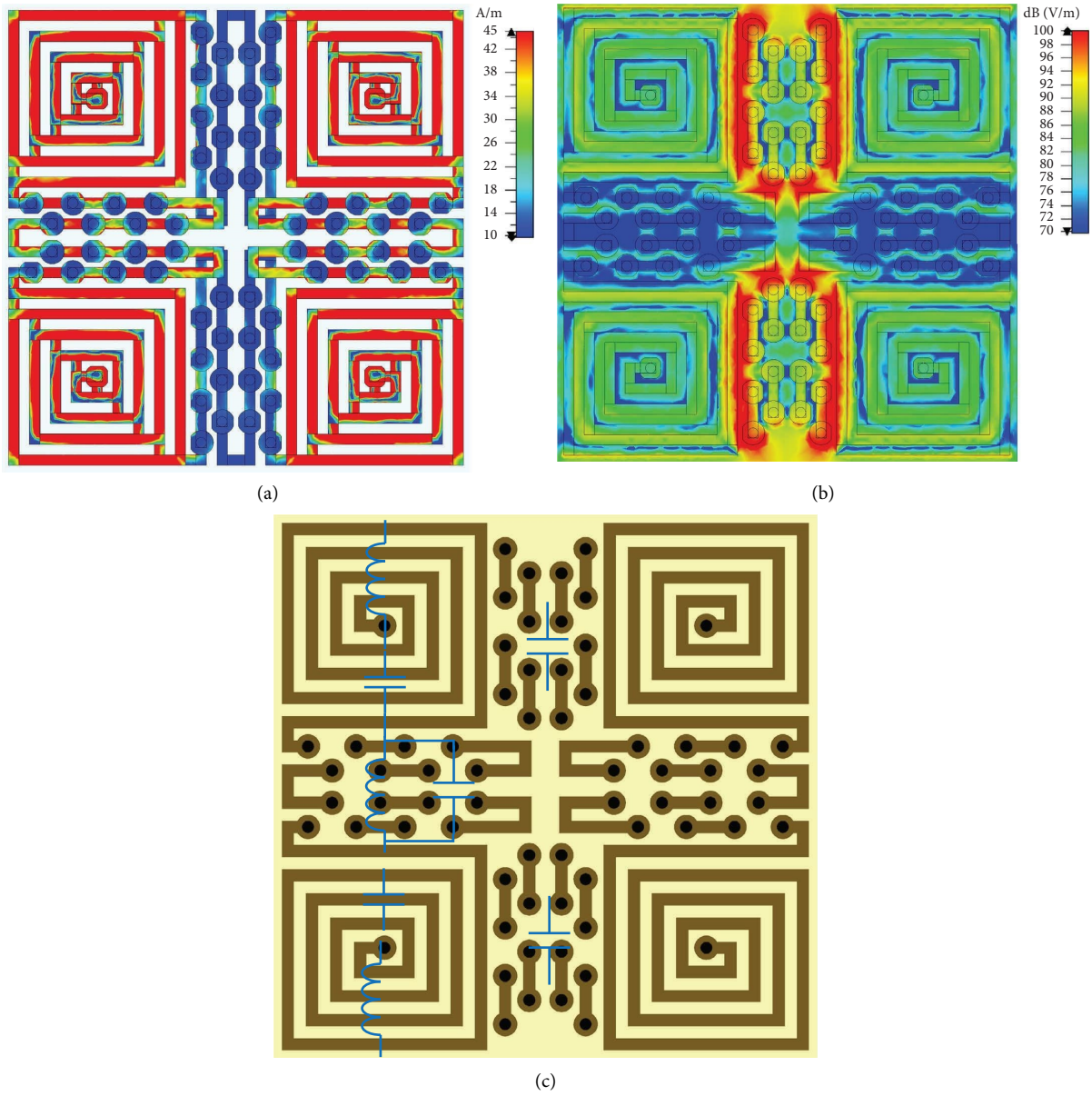

Figure 5: Surface current and electric field distribution at the bottom under TE mode excitation. (a) Surface current. (b) Electric field. (c) Relative positions of the inductors and capacitors on the FSS.

Therefore, after the proper combination and simplification of the capacitor and inductor, a simplified equivalent circuit model is obtained as shown in Figure 6(b). This model helps to further obtain the specific values of LC, and subsequent discussions will use this simplified model.

Further analysis of this simplified equivalent circuit model, i.e., the impedance of the model can be expressed as follows [25, 26].

$$Z_{FSS} = \frac{1}{\left(1/\left(j\omega L_2'/j\omega C_2'\right)\left(j\omega L_2' + 1/j\omega C_2'\right) + \left(j\omega L_1' + 1/j\omega C_1'\right)\right) + j\omega C_3'}. \quad (1)$$

For equation (1), the solution corresponding to the zero point is also the resonant frequency of the FSS. Expanding and simplifying the above equation, the solution of its zero point should satisfy the following equation.

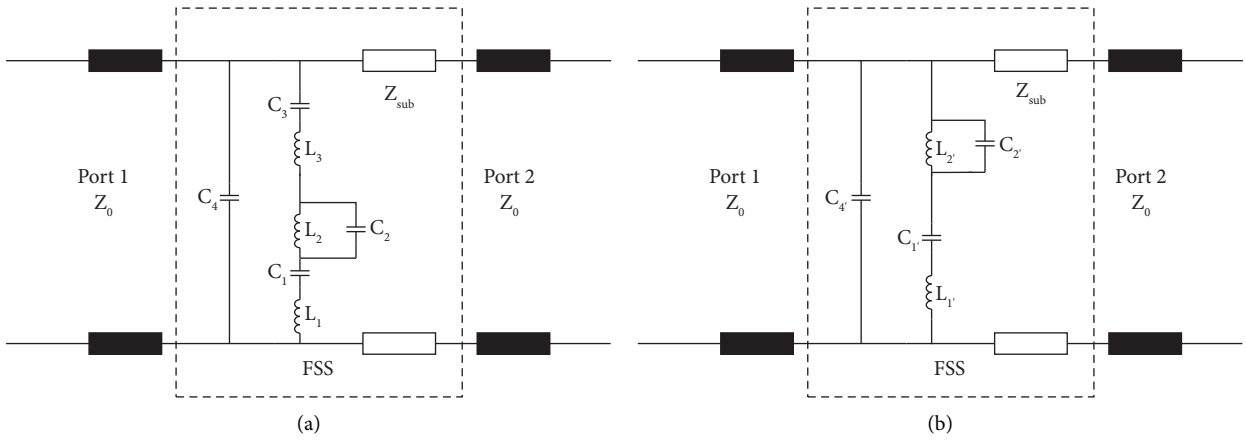

Figure 6: An equivalent circuit and its simplified model. (a) The equivalent circuit. (b) The simplified circuit.

$$\frac{l_1' + l_2'}{C_2'} + \frac{l_2'}{C_1'} = \omega^2 l_1' l_2' + \frac{1}{\omega^2 C_1' C_2'}. \tag{2}$$

A further solution of equation (2) results in the resonant frequency f.

$$f_{FSS} = \frac{1}{2\pi} \sqrt{\frac{(L_1' + L_2')C_1' + L_2'C_2' - \sqrt{((L_1' + L_2')C_1' + L_2'C_2')^2 - 4L_1'L_2'C_1'C_2'}}{2L_1'L_2'C_1'C_2'}}. \tag{3}$$

The specific values of the components in the circuit can be obtained with curve fitting by using Keysight ADS. Figure 7 shows the transmission coefficients of the FSS. In this case, $L_1' = 49.398$ nH, $L_2' = 35.574$ nH, $C_1' = 0.312$ pF, $C_2' = 0.420$pF, and $C_4' = 0.245$pF. The ECM results are very close to the full-wave simulation, and there is almost no difference between the resonant frequencies of them, while the ECM has a deeper depression in coefficients, which is caused by the fact that the losses of the dielectric and metal are not considered in the ECM. Therefore, with the benefit that the circuit simulation time is much shorter than that of the full-wave simulation, the proposed equivalent circuit can be used for more efficient and convenient analysis of the FSS and can better guide the design.

4. Experimental Results

In order to verify the proposed design, the FSS is fabricated and measured. An FR4 dielectric substrate is used, whose total size is 702 mm × 702 mm with 104 × 104 cells arranged, and the parameters of one cell are the same as in Figure 1. The experimental results are obtained using the free-space measurement method. In the microwave anechoic chamber, two horn antennas are used as the transmitting and receiving antennas, respectively, and the distance between them is 3.5 m. The FSS is placed on the front side of the receiving antenna, and the test environment is as shown in Figure 8.

The performance of the FSS with different incident angles is tested in the TE and TM polarization modes, respectively, and the measured S-parameters are shown in Figure 9. It can be found that although the measured deviation forms the simulation, the offset of the resonant frequency is still very small when the angle change reaches 85 degrees, and the maximum offset is less than 10 MHz. The high angular stability is demonstrated, which is in good agreement with the simulation results. The small inaccuracy may be caused by the error of fabrication or the loss of dielectric. The FSS performance at different polarization angles was also tested by rotating the FSS to change the phi. The measured transmission coefficients from 0 to 60 degrees of polarization angle are given in Figure 9. Similar to the previous simulation results, the insensitivity of the transmission coefficients to the polarization angle is shown, i.e., a better polarization stability.

To further demonstrate the performance of the designed FSS, Table 1 represents the performance of the proposed FSS in this paper compared with some recently published band-stop FSSs.

5. Extension of the Proposed Structure

The proposed two-layer FSS structure could be extended to an N-layer structure by adding layers on either the top or bottom side. Figure 10 shows the expanded FSS structure at three layer and four layer, and in this case, the cell size and the total thickness of the FSS do not change.

By increasing the number of layers of the PCB, more vias and longer lengths of metal strips can be added, which allows the LC to continue to increase and enable further miniaturization. As can be seen from the figure, the increase to

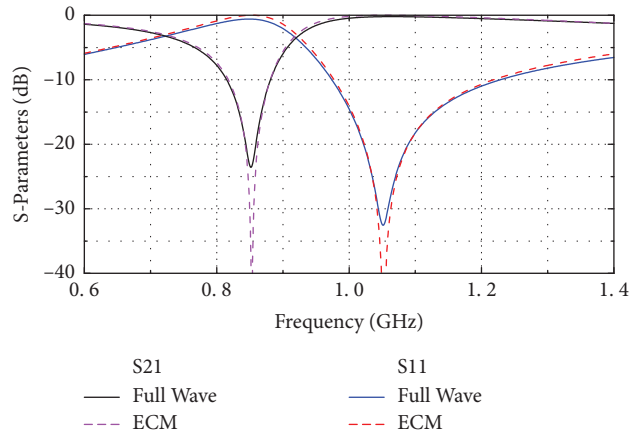

Figure 7: S-parameters under full-wave and ECM simulation.

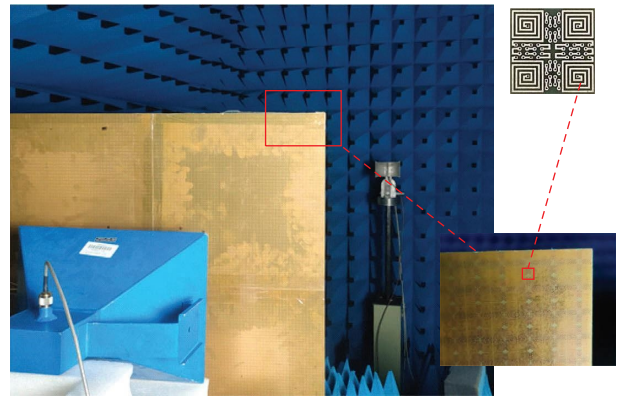

Figure 8: Fabricated FSS with the measurement setup.

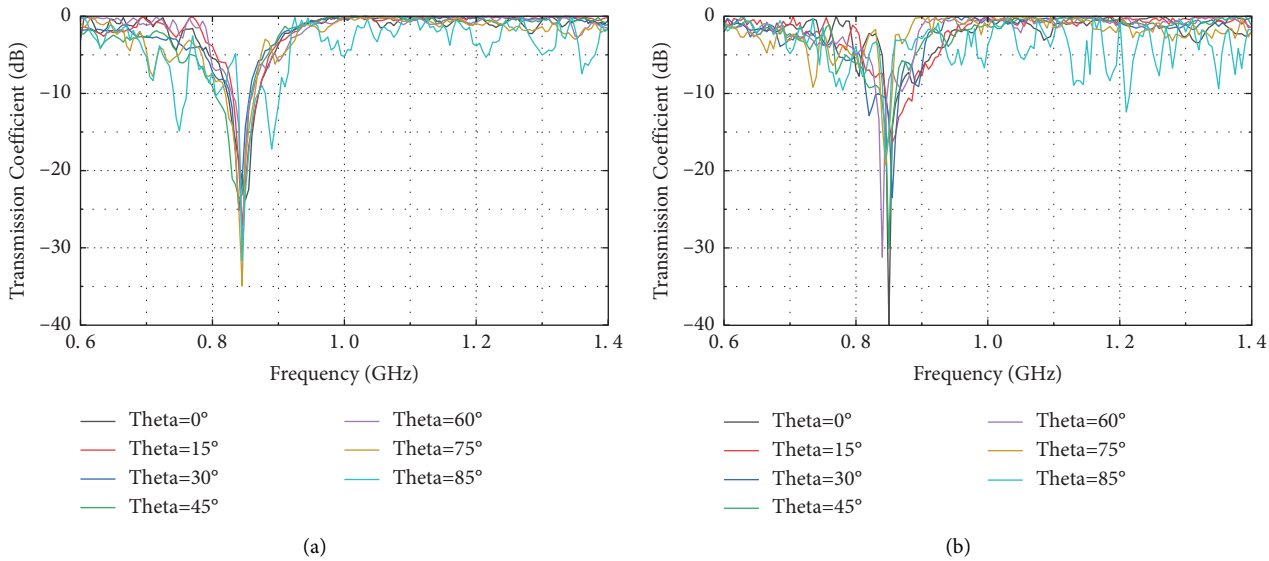

Figure 9: Continued.

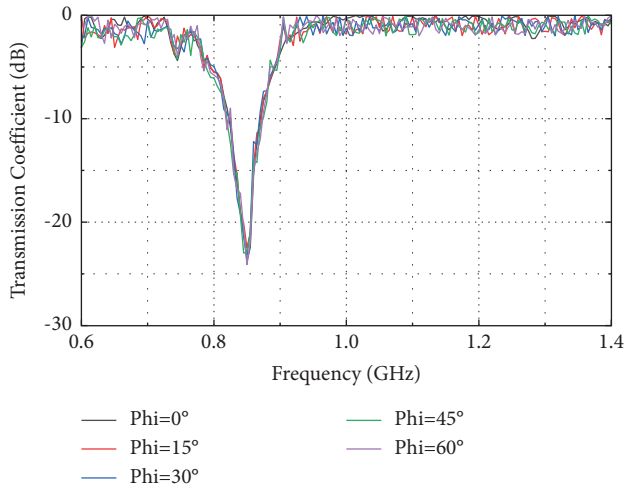

(c)

Figure 9: Measured transmission coefficients of the proposed FSS. (a) Various incident angles of the TE mode. (b) Various incident angles of the TM mode. (c) Various polarization angles.

Table 1: Comparison of the proposed miniaturized FSS with reported structures.

References	Resonant frequency	Material characters	Size of unit cell (λ_0^2)	Thickness of FSS structure (λ_0)	Angular stability (degree)	Miniaturization technique
[10]	1.66 GHz	FR-4, $\varepsilon_r = 4.3$	0.02×0.02	0.009	75	2.5-D structure made of square spirals
[13]	900 MHz	FR-4, $\varepsilon_r = 4.3$	0.021×0.021	0.005	80	2.5D closed loop
[14]	1.44 GHz	F4B, $\varepsilon_r = 4.4$	0.022×0.022	0.018	60	Handshake convoluted stripe
[16]	1.056 GHz	FR-4, $\varepsilon_r = 4.3$	0.034×0.034	0.006	75	Four-legged loaded loop elements
[18]	1.1 GHz	FR-4, $\varepsilon_r = 4.4$	0.022×0.022	0.006	60	Meandered lines
This work	850 MHz	FR-4, $\varepsilon_r = 4.6$	0.019×0.019	0.003	85	Novel 2.5D closed loop

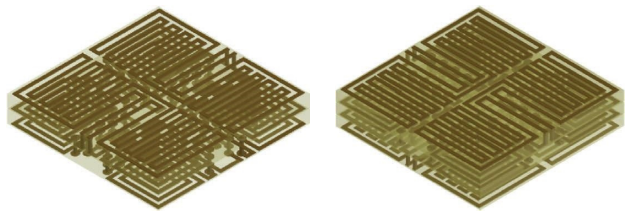

(a) (b)

Figure 10: Multiple layer structure for the proposed FSS. (a) Three layers. (b) Four layers.

three layers requires only a slight change to the original top layer structure to add two more vias and an additional new top layer using the meandering line structure at which point, the bottom layer does not need to be changed in any way. At this point, the structure is actually still a closed loop, so it can be increased to four or more layers in a similar way.

Figure 11 gives the S-parameters of the expanded three-layer and four-layer PCB structure under full-wave simulation. From the results, it can be seen that its resonant frequency is further reduced to 470 MHz. Thus, by varying the number of PCB layers in this section and the dielectric constant and board thickness as mentioned in section 2, the

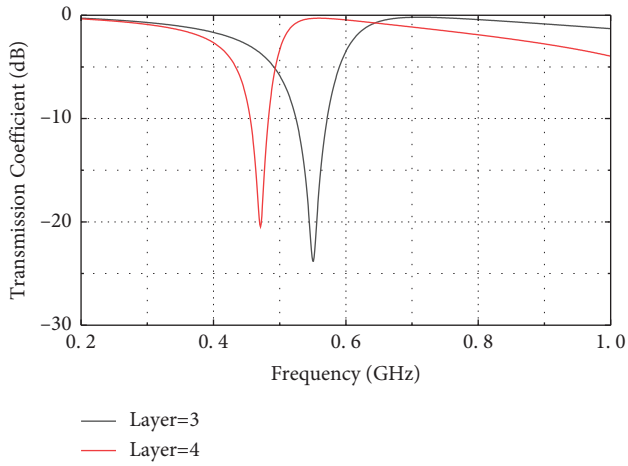

Figure 11: Transmission coefficients of the extension structure for the proposed FSS.

proposed FSS can be designed to the resonant frequency desired and still maintain excellent miniaturization.

6. Conclusion

A miniaturized FSS with high angular stability is proposed, and the design and demonstration process are elaborated. The designed unit cell is $0.019\lambda_0 \times 0.019\lambda_0$ with a thickness of $0.003\lambda_0$. Its stability is maintained in both the TE and TM modes by varying the incident angle up to 85 degrees. At the same time, the equivalent circuit model of the FSS and the values of each lumped element are given. It is verified that the equivalent circuit simulation results are in good accordance with the full-wave simulation results, and the FSS performance can be analyzed more efficiently with the equivalent circuit model. The optimized FSS has a resonant frequency of 850 MHz, and as a band-stop FSS, it can be applied as an electromagnetic shield for GSM850. A prototype of the FSS is also fabricated and measured, proving a good agreement with the simulation results.

Data Availability

The data generated or used during the study are included within the article.

Conflicts of Interest

The authors declare that they have no conflicts of interest.

Acknowledgments

This work was supported in part by the National Natural Science Foundation of China under Grant 61731007.

References

[1] M. Bilal, R. Saleem, Q. H. Abbasi, B. Kasi, and M. F. Shafique, "Miniaturized and flexible FSS-based EM shields for conformal applications," *IEEE Transactions on Electromagnetic Compatibility*, vol. 62, no. 5, pp. 1703–1710, 2020.

[2] F. Erkmen, T. S. Almoneef, and O. M. Ramahi, "Scalable electromagnetic energy harvesting using frequency-selective surfaces," *IEEE Transactions on Microwave Theory and Techniques*, vol. 66, no. 5, pp. 2433–2441, 2018.

[3] A. Chandra, N. Mishra, R. Kumar, K. Kumar, and H. Y. Patil, "A superstrate and FSS embedded dual band waveguide aperture array with improved far-field characteristics," *Microwave and Optical Technology Letters*, vol. 65, no. 1, pp. 341–347, 2023.

[4] W. Liao, W. Zhang, Y. Hou, S. Chen, C. Y. Kuo, and M. Chou, "An FSS-integrated low-RCS radome design," *IEEE Antennas and Wireless Propagation Letters*, vol. 18, no. 10, pp. 2076–2080, 2019.

[5] M. J. Qu, Y. F. Feng, J. X. Su, and S. M. A. Shah, "Design of a single-layer frequency selective surface for 5G shielding," *IEEE Microwave and Wireless Components Letters*, vol. 31, no. 3, pp. 249–252, 2021.

[6] S. Cho, S. Yoon, and I. Hong, "Design of three-dimensional frequency selective structure with replaceable unit structures using a 3-D printing technique," *IEEE Antennas and Wireless Propagation Letters*, vol. 17, no. 11, pp. 2041–2045, 2018.

[7] Y. Ma, X. Zhang, S. Wu, Y. Yuan, and N. Yuan, "A hybrid 2-D–3-D miniaturized multiorder wide bandpass FSS," *IEEE Antennas and Wireless Propagation Letters*, vol. 21, no. 2, pp. 307–311, 2022.

[8] B. Sanz-Izquierdo and E. A. Parker, "3-D printing of elements in frequency selective arrays," *IEEE Transactions on Antennas and Propagation*, vol. 62, no. 12, pp. 6060–6066, 2014.

[9] Y.-M. Yu, C.-N. Chiu, Y.-P. Chiou, and T.-L. Wu, "An effective via-based frequency adjustment and minimization methodology for single-layered frequency-selective surfaces," *IEEE Transactions on Antennas and Propagation*, vol. 63, no. 4, pp. 1641–1649, 2015.

[10] Y.-M. Yu, C.-N. Chiu, Y.-P. Chiou, and T.-L. Wu, "A novel 2.5-dimensional ultraminiaturized-element frequency selective surface," *IEEE Transactions on Antennas and Propagation*, vol. 62, no. 7, pp. 3657–3663, 2014.

[11] D. Li, T. Li, E. Li, and Y. Zhang, "A 2.5-D angularly stable frequency selective surface using via-based structure for 5G EMI shielding," *IEEE Transactions on Electromagnetic Compatibility*, vol. 60, no. 3, pp. 768–775, 2018.

[12] Y.-M. Yu, C.-N. Chiu, Y.-P. Chiou, and T.-L. Wu, "A novel 2.5-dimensional ultraminiaturized-element frequency selective surface," *IEEE Transactions on Antennas and Propagation*, vol. 62, no. 7, pp. 3657–3663, 2014.

[13] Y.-M. Yu, C.-N. Chiu, Y.-P. Chiou, and T.-L. Wu, "An effective via-based frequency adjustment and minimization methodology for single-layered frequency-selective surfaces," *IEEE Transactions on Antennas and Propagation*, vol. 63, no. 4, pp. 1641–1649, 2015.

[14] M. W. Niaz, Y. Yin, S. Zheng, L. Zhao, and J. Chen, "Design and analysis of an ultraminiaturized FSS using 2.5-D convoluted square spirals," *IEEE Transactions on Antennas and Propagation*, vol. 68, no. 4, pp. 2919–2925, 2020.

[15] M. W. Niaz, Y. Yin, and J. Chen, "Synthesis of ultraminiaturized frequency-selective surfaces utilizing 2.5-D tapered meandering lines," *IEEE Antennas and Wireless Propagation Letters*, vol. 19, no. 1, pp. 163–167, 2020.

[16] Y. Shi, W. Zhuang, W. Tang, C. Wang, and S. Liu, "Modeling and analysis of miniaturized frequency-selective surface based on 2.5-dimensional closed loop with additional transmission pole," *IEEE Transactions on Antennas and Propagation*, vol. 64, no. 1, pp. 346–351, 2016.

[17] Y. Shi, W. Tang, W. Zhuang, and C. Wang, "Miniaturised frequency selective surface based on 2.5-dimensional closed loop," *Electronics Letters*, vol. 50, no. 23, pp. 1656–1658, 2014.

[18] M. Chaluvadi, V. K. Kanth, and K. G. Thomas, "Design of a miniaturized 2.5-D frequency selective surface with angular incidence and polarization stability," *IEEE Transactions on Electromagnetic Compatibility*, vol. 62, no. 4, pp. 1068–1075, 2020.

[19] T. Hong, K. Peng, and M. Wang, "Miniaturized frequency selective surface using handshake convoluted stripe," *IEEE Antennas and Wireless Propagation Letters*, vol. 18, no. 10, pp. 2026–2030, 2019.

[20] T. Hussain, Q. Cao, J. K. Kayani, and I. Majid, "Miniaturization of frequency selective surfaces using 2.5-D knitted structures: design and synthesis," *IEEE Transactions on Antennas and Propagation*, vol. 65, no. 5, pp. 2405–2412, 2017.

[21] L. Murugasamy and R. Sivasamy, "A novel fractal inspired iterated four-legged loaded loop elements based 2.5-D miniaturized frequency selective surface," *IEEE Transactions on Electromagnetic Compatibility*, vol. 63, no. 6, pp. 2164–2167, 2021.

[22] S. Khajevandi, H. Oraizi, A. Amini, and M. Poordaraee, "Design of miniaturised-element FSS based on 2.5-dimensional closed-loop Hilbert fractal," *IET Microwaves, Antennas & Propagation*, vol. 13, no. 6, pp. 742–747, 2019.

[23] B. Ashvanth, B. Partibane, and M. G. N. Alsath, "An ultra-miniaturized frequency selective surface with angular and polarization stability," *IEEE Antennas and Wireless Propagation Letters*, vol. 21, no. 1, pp. 114–118, 2022.

[24] R. K. Singh, A. Gupta, A. Sharma, U. Tyagi, N. Gupta, and A. Yadav, "An ultra-thin quad-band metamaterial inspired absorber using symmetric bent-arrow shaped resonator for sensing and imaging in defense applications," *Materials Research Express*, vol. 7, no. 11, Article ID 115801, 2020.

[25] F. Costa, A. Monorchio, and G. Manara, "Efficient analysis of frequency-selective surfaces by a simple equivalent-circuit model," *IEEE Antennas and Propagation Magazine*, vol. 54, no. 4, pp. 35–48, 2012.

[26] P.-C. Zhao, Z.-Y. Zong, W. Wu, B. Li, and D.-G. Fang, "An FSS structure with geometrically separable meander-line inductors and parallel-plate capacitors," *IEEE Transactions on Antennas and Propagation*, vol. 65, no. 9, pp. 1–4705, 2017.